

# NUCLEAR ASYMMETRY ENERGY AND ISOVECTOR STIFFNESS WITHIN THE EFFECTIVE SURFACE APPROXIMATION

J.P. Blocki,<sup>1</sup> A.G. Magner<sup>a,2</sup> P. Ring,<sup>3</sup> and A.A. Vlasenko<sup>4</sup>

<sup>1</sup>*National Centre for Nuclear Research, Otwock 05-400, Poland*

<sup>2</sup>*Institute for Nuclear Research, Kyiv 03680, Ukraine*

<sup>3</sup>*Technical Munich University, D-85747 Garching, Germany*

<sup>4</sup>*National Technical University of Ukraine "KPI", Kyiv 03056, Ukraine*

The isoscalar and isovector particle densities and the surface tension coefficients at the average binding energy are used to derive analytical expressions of the neutron skin thickness and the isovector stiffness of sharp edged proton-neutron asymmetric nuclei. For most Skyrme forces these quantities are significantly larger than the well known ones. Using the analytical isovector surface energy constants in the framework of the hydrodynamical and the Fermi-liquid droplet models the mean energies and the sum rules of the isovector giant dipole resonances are in fair agreement with the experimental data.

**Keywords:** Nuclear binding energy, liquid droplet model, extended Thomas-Fermi approach, nuclear surface energy, symmetry energy, neutron skin thickness, isovector stiffness.

PACS numbers: 21.10.Dr, 21.65.Cd, 21.60.Ev, 21.65.Ef

## I. INTRODUCTION

A simple and accurate solution of the particle density distributions was obtained within the nuclear effective surface (ES) approximation in Refs. [1–3]. It exploits the saturation properties of nuclear matter in the narrow diffuse-edge region in finite heavy nuclei. The ES is defined as the location of points with a maximum density gradient. An orthogonal coordinate system related locally to the ES is specified by the distance  $\xi$  of a given point from this surface and tangent coordinates  $\eta$  parallel to the ES (see Fig. 1). Using nuclear energy density functional theory the variational condition derived from minimizing the nuclear energy at some fixed integrals of motion is simplified in the  $\xi, \eta$  coordinates. In particular, in the extended Thomas-Fermi (ETF)

<sup>a</sup> magner@kinr.kiev.ua

approach [4], it can be done for any fixed deformation using the expansion in a small parameter  $a/R \sim A^{-1/3} \ll 1$  for heavy enough nuclei where  $a$  is of the order of the diffuse edge thickness of the nucleus,  $R$  is the mean curvature radius of the ES, and  $A$  is the number of nucleons. The accuracy of the ES approximation in the ETF approach without spin-orbit (SO) and asymmetry terms was checked [3] by comparing results with those of the Hartree-Fock (HF) and ETF theories for some Skyrme forces. The ES approach [3] was also extended by taking into account the SO and asymmetry effects [5].

In the present work, solutions for the isoscalar and isovector particle densities and energies in the ES approximation of the ETF approach are applied to analytical calculations of the neutron skin and isovector stiffness coefficient in the leading order of the parameter  $a/R$  (see also Ref. [6]). Our results are compared with older investigations [7–10] in the liquid droplet model (LDM) and with more recent works [11–19]. We suggest to study also the splitting of the isovector giant dipole resonances into the main and satellite (pygmy) peaks [18, 19] as a function of the analytical isovector surface energy constant of the ES approach within the Fermi-liquid droplet (FLD) model [20–22]. The analytical expressions for the surface symmetry energy constants are tested by the mean energies of the isovector giant dipole resonances (IVGDR) within the hydrodynamical (HD) and FLD models.

The manuscript is organized as follows: In section II we give an outlook of the basic points of the ES approximation within the density functional theory and main results for the isoscalar and isovector particle densities. Section III is devoted to analytical derivations of the symmetry energy in terms of the surface energy coefficient, the neutron skin thickness and the isovector stiffness. The discussions of the results are given in section IV and summarized in section V. Some details of our calculations are presented in Appendixes A, B and C.

## II. ENERGY AND PARTICLE DENSITIES

We start with the nuclear energy as a functional of the isoscalar and the isovector densities  $\rho_{\pm} = \rho_n \pm \rho_p$ :

$$E = \int d\mathbf{r} \mathcal{E}(\rho_+, \rho_-) , \quad (1)$$

in the local density approach [4, 23–27] with the energy density  $\mathcal{E}(\rho_+, \rho_-)$ ,

$$\begin{aligned} \mathcal{E}(\rho_+, \rho_-) \approx & -b_V \rho_+ + JI^2 \rho_+ + \rho_+ [\varepsilon_+(\rho_+) - \varepsilon_-(\rho_+, \rho_-)] + \\ & + (\mathcal{C}_+ + \mathcal{D}_+ \rho_+) (\nabla \rho_+)^2 + (\mathcal{C}_- + \mathcal{D}_- \rho_+) (\nabla \rho_-)^2 , \end{aligned} \quad (2)$$

where  $I = (N - Z)/A$  is the asymmetry parameter,  $N = \int d\mathbf{r} \rho_n(\mathbf{r})$  and  $Z = \int d\mathbf{r} \rho_p(\mathbf{r})$  are the neutron and proton numbers and  $A = N + Z$ . As usual, the energy density  $\mathcal{E}$  in Eq. (2) contains the volume part given by the first two terms of Eq. (2) and the surface part including the density gradients [1, 3]. The particle separation energy  $b_v \approx 16$  MeV and the symmetry energy constant of the nuclear matter  $J \approx 30$  MeV specify the volume terms in Eq. (2). Eq. (2) can be applied in a semiclassical approximation for realistic Skyrme forces [23–27], in particular by neglecting higher  $\hbar$  corrections in the ETF kinetic energy [2–4] and Coulomb terms. Up to small Coulomb exchange terms they all can be easily taken into account (see Refs. [1, 3, 5]). The constants  $\mathcal{C}_\pm$  and  $\mathcal{D}_\pm$  are defined by the parameters of the Skyrme forces [23, 24]. The isoscalar part of the surface energy-density which does not depend explicitly on the density gradient terms, is determined by the function  $\varepsilon_+(\rho_+)$  [3, 5] which satisfies the saturation condition:  $\varepsilon_+(\bar{\rho}) = 0$ ,  $d\varepsilon_+(\bar{\rho})/d\rho_+ = 0$ , where  $\bar{\rho} = 3/4\pi r_0^3 \approx 0.16 \text{ fm}^{-3}$  is the density of the infinite nuclear matter and  $r_0 = R/A^{1/3}$  is the radius constant. Here we use a quadratic approximation  $\varepsilon_+ = K(\rho_+ - \bar{\rho})^2/(18\bar{\rho}^2)$ , where  $K$  is the incompressibility modulus of symmetric nuclear matter, mainly  $K \approx 220 - 260$  MeV (see Table I). The isovector component can be simply evaluated as  $\varepsilon_- = J(I^2 - \rho_-^2/\rho_+^2)$  [5]. The isoscalar SO gradient terms in Eq. (2) are defined with a constant:  $\mathcal{D}_+ = -9mW_0^2/16\hbar^2$ , where  $W_0 \approx 100 - 130 \text{ MeV}\cdot\text{fm}^5$  and  $m$  is the nucleon mass [4, 23–26].

Minimizing the energy  $E$  under the constraints of the fixed particle number  $A = \int d\mathbf{r} \rho_+(\mathbf{r})$  and neutron excess  $N - Z = \int d\mathbf{r} \rho_-(\mathbf{r})$  (also others like a deformation [1, 3]) one arrives at the Lagrange equations with the corresponding multipliers,  $\lambda_+$  and  $\lambda_-$  being the isoscalar and isovector chemical potentials, respectively (see Appendixes A and B). Our approach can be applied for any deformation parameter of the nuclear surface if its diffuseness with respect to the curvature radius  $a/R$  is small. The analytical solutions will be obtained approximately up to the order of  $A^{2/3}$  in the binding energy. To satisfy the condition of the particle number conservation with the required accuracy we account for relatively small surface corrections ( $\propto a/R \sim A^{-1/3}$  at the first order) to the leading terms in the Lagrange multipliers [2, 3, 5] (Appendixes B and C).

For the isoscalar particle density,  $w = \rho_+/\bar{\rho}$  one has up to *leading* terms in the parameter  $a/R$  the usual first-order differential Lagrange equation with the solution [3, 5]

$$x = - \int_{w_r}^w dy \sqrt{\frac{1 + \beta y}{y\epsilon(y)}}, \quad x = \frac{\xi}{a}, \quad a = \sqrt{\frac{\mathcal{C}_+ \bar{\rho} K}{30 b_v^2}}, \quad (3)$$

where  $\beta = \mathcal{D}_+ \bar{\rho}/\mathcal{C}_+$  is the dimensionless SO parameter. For convenience we introduced also the dimensionless parameter  $\epsilon = 18\varepsilon/K$ . For  $w_r = w(x = 0)$  one has the boundary condition,

$d^2w(x)/dx^2 = 0$  at the ES ( $x = 0$ ):

$$\epsilon(w_r) + w_r(1 + \beta w_r) [d\epsilon(w_r)/dw] = 0 . \quad (4)$$

In Eq. (3),  $a \approx 0.5 - 0.6$  fm is the diffuseness parameter as shown in Table I [ $\xi = (r - R)/a$  for spherical nuclei in the spherical coordinates]. The diffuseness of the edge  $a_d$  is given by

$$a_d = \sqrt{5(\overline{\xi^2} - \bar{\xi}^2)/3} = a\sqrt{5(\overline{x^2} - \bar{x}^2)/3}, \quad \bar{x}^n = \int_{-\infty}^{\infty} x^n dx (dw/dx), \quad (5)$$

where bars mean an averaging with the surface density distribution  $dw/dx$  [3]. For all Skyrme forces (Table I) the parameter  $a$  introduced in Eq. (3) measures the diffuseness of the nuclear edge as the mean-squared fluctuation of  $\xi$  due to the relation  $a_d \approx a\sqrt{5/3}$  (see also Refs. [3, 15]). As shown in Ref. [5], the influence of the semiclassical  $\hbar$  corrections (related to the ETF kinetic energy) to  $w(x)$  is negligibly small everywhere, besides the quantum tail outside the nucleus ( $x \gtrsim 1$ ). Therefore, all these corrections were neglected in Eq. (2). With a good convergence of the expansion of the  $\epsilon(y)$  in powers of  $1 - y$  up to the quadratic term [3, 5],  $\epsilon = (1 - y)^2$ , one finds the analytical solutions of Eq. (3) in terms of the algebraic, trigonometric and logarithmic functions [see Eq. (A3)]. For  $\beta = 0$  (i.e. without SO terms), it simplifies to the solution  $w(x) = \tanh^2[(x - x_0)/2]$  for  $x \leq x_0 = 2\text{arctanh}(1/\sqrt{3})$  and zero for  $x$  outside the nucleus ( $x > x_0$ ).

For the isovector density,  $w_-(x) = \rho_-/(\bar{\rho}I)$ , after simple transformations of the isovector Lagrange equation up to the leading term in  $a/R$  in the ES approximation one similarly finds the equation and boundary condition [see Eq. (A2)]. The analytical solution for  $w_- = w\cos[\psi(w)/\sqrt{1+\beta}]$  can be obtained through the expansion (A5) of  $\psi$  in powers of

$$\tilde{w}(w) = (1 - w)/c_{sym} \quad \text{with} \quad c_{sym} = a \sqrt{\frac{J}{\bar{\rho} |\mathcal{C}_-|}}. \quad (6)$$

Expanding up to the second order in  $\tilde{w}$  one finds (Appendix A)

$$w_- = w \left( 1 - \frac{\psi^2(w)}{2(1+\beta)} \right), \quad \psi(w) = \tilde{w}(w) [1 + \tilde{c}\tilde{w}(w)], \quad \tilde{c} = \frac{\beta c_{sym}/2 - 1}{1 + \beta}. \quad (7)$$

In Fig. 2 the SO dependence of the function  $w_-(x)$  is compared with that of the density  $w(x)$  for the SLy7 force as a typical example [5]. In particular, as seen in Figs. 3 and 4 the isoscalar  $w(x)$  and the isovector  $w_-(x)$  densities depend only rather weakly on the most of the Skyrme forces [23, 24]. Only in a larger (logarithmic) scale, as shown in Fig. 4, one observes notable differences in the isovector densities  $w_-$  derived from different Skyrme forces within the edge diffuseness.

### III. ISOVECTOR ENERGY AND STIFFNESS

Within the improved ES approximation where also higher order corrections in the small parameter  $a/R$  are taken into account we derive equations for the nuclear surface itself (see Appendix

B and Refs. [2, 3, 5]). For more exact isoscalar and isovector particle densities we account for the main terms in the next order of the parameter  $a/R$  in the Lagrange equations [cf. Eq. (B1) as compared with Eq. (A1)]. Multiplying these equations by  $\partial\rho_-/\partial\xi$  and integrating them over the ES in the normal-to-surface direction  $\xi$  and using the solutions for  $w_{\pm}(x)$  up to the leading orders [see Eqs. (3) and (7)] one arrives at the ES equations in the form of the macroscopic boundary conditions (B2) [1–3, 5, 22, 28–30]. They ensure equilibrium through the equivalence of the volume and surface (capillary) pressure (isoscalar or isovector) variations. As shown in Appendix B, the latter ones are proportional to the corresponding surface tension coefficients:

$$\sigma_{\pm} = b_S^{(\pm)}/4\pi r_0^2, \quad b_S^{(\pm)} \approx 8\pi r_0^2 \mathcal{C}_{\pm} \int_{-\infty}^{\infty} d\xi \left(1 + \frac{\mathcal{D}_{\pm}}{\mathcal{C}_{\pm}} \rho_{\pm}\right) \left(\frac{\partial\rho_{\pm}}{\partial\xi}\right)^2. \quad (8)$$

The nuclear energy  $E$  (equation (1)) in this improved ES approximation (Appendix C) is split into volume and surface (both with the symmetry) terms,

$$E \approx -b_V A + J(N - Z)^2/A + E_S. \quad (9)$$

For the surface energy  $E_S$  one obtains

$$E_S = E_S^{(+)} + E_S^{(-)} \quad (10)$$

with the following isoscalar (+) and isovector (-) surface components:

$$E_S^{(\pm)} = \sigma_{\pm} \mathcal{S} = b_S^{(\pm)} \mathcal{S}/(4\pi r_0^2), \quad (11)$$

where  $\mathcal{S}$  is the surface area of the ES. The energies  $E_S^{(\pm)}$  in Eq. (11) are determined by the isoscalar  $b_S^{(+)}$  and isovector  $b_S^{(-)}$  surface energy constants of Eq. (8). These constants are proportional to the corresponding surface tension coefficients  $\sigma_{\pm}$  in Eq. (8) through the solutions (3) and (7) for  $\rho_{\pm}(\xi)$  which can be taken into account in leading order of  $a/R$  (Appendix C). These coefficients  $\sigma_{\pm}$  are the same as found in the expressions for the capillary pressures of the boundary conditions (B2).

For the energy surface coefficients  $b_S^{(\pm)}$  one obtains

$$b_S^{(+)} = \frac{6\mathcal{C}_+ \bar{\rho} \mathcal{J}_+}{r_0 a}, \quad \mathcal{J}_+ = \int_0^1 dw \sqrt{w(1 + \beta w) \epsilon(w)}, \quad (12)$$

$$b_S^{(-)} = k_S I^2, \quad k_S = 6\bar{\rho} \mathcal{C}_- \mathcal{J}_-/(r_0 a), \quad (13)$$

$$\mathcal{J}_- = -\frac{1}{1 + \beta} \int_0^1 (1 - w)^2 dw \sqrt{\frac{w(1 + \beta w)}{\epsilon(w)}} (1 + \tilde{c}w)^2. \quad (14)$$

For  $\tilde{w}$  and  $\tilde{c}$ , see Eqs. (6) and (7), respectively. Simple expressions for the constants  $b_S^{(\pm)}$  in Eqs. (12) and (13) can be easily derived in terms of algebraic and trigonometric functions by calculating

explicitly the integrals over  $w$  for the quadratic form of  $\epsilon(w)$  [Eqs. (C3) and (C4)]. Note that in these derivations we neglected curvature terms and, being of the same order, shell corrections. The isovector energy terms were obtained within the ES approximation with high accuracy up to the product of two small quantities,  $I^2$  and  $(a/R)^2$ .

According to the theory [7–9], one may define the isovector stiffness  $Q$  with respect to the difference  $R_n - R_p$  between the neutron and proton radii as a collective variable,

$$E_s^{(-)} = -\frac{\bar{\rho}r_0}{3} \oint dS Q \tau^2 \approx -\frac{Q \tau^2 \mathcal{S}}{4\pi r_0^2}, \quad \tau = \frac{R_n - R_p}{r_0}, \quad (15)$$

where  $\tau$  is the neutron skin. Comparing this expression with Eq. (11) for the isovector surface energy written through the isovector surface energy constant  $b_s^{(-)}$  [Eq. (13)], one obtains

$$Q = -b_s^{(-)}/\tau^2 = -k_S I^2/\tau^2. \quad (16)$$

Defining the neutron and proton radii  $R_{n,p}$  as the positions of the maxima of the neutron and proton density gradients, respectively,

$$\left( \frac{\partial^2 \rho_{n,p}}{\partial r^2} \right)_{r=R_{n,p}} = 0, \quad \left( \frac{\partial^2 \rho_+}{\partial r^2} \right)_{r=R} = 0, \quad (17)$$

we use the expansion in small values of  $\delta R_{n,p} = R_{n,p} - R$  near the ES. Thus, in the linear approximation in  $\delta R_{n,p}$  and  $I$  one obtains

$$\tau = -2 \frac{aI}{r_0} \frac{\partial^2 w_-}{\partial x^2} \Big|_{x=0} \left( \frac{\partial^3 w}{\partial x^3} \Big|_{x=0} \right)^{-1} = \frac{8aI}{r_0 c_{sym}^2} g(w_r), \quad (18)$$

where

$$g(w) = \frac{w^{3/2}(1 + \beta w)^{5/2}}{(1 + \beta)(3w + 1 + 4\beta w)} \left\{ w(1 + 2\tilde{c}\tilde{w})^2 + 2\tilde{w}(1 + \tilde{c}\tilde{w})[\tilde{c}w - c_{sym}(1 + 2\tilde{c}\tilde{w})] \right\}, \quad (19)$$

and  $w_r$  is the solution of the boundary equation (4). In the derivations of Eq. (18), we used the approximation  $\epsilon(w) = (1 - w)^2$  and expressions (3) for  $w(x)$  and (7) for  $w_-(x)/w$ . The neutron and proton particle-density variations in Eq. (17) conserve the center of mass in the same linear approximation in  $\delta R_{n,p}$  and  $I$ . Inserting Eqs. (18) and (13) into Eq. (16) one finally arrives at

$$Q = -\nu \frac{J^2}{k_S}, \quad \nu = \frac{k_S^2 I^2}{\tau^2 J^2} = \frac{9\mathcal{J}_-^2}{16g^2(w_r)}, \quad (20)$$

where  $\mathcal{J}_-$  and  $g(w_r)$  are given by Eqs. (14), (19) and (4). In the derivation of Eq. (20) we used also Eq. (3) for the diffuseness parameter  $a$  and Eq. (6) for the  $c_{sym}$ . Note that  $Q = -9J^2/4k_S$  has been predicted in Refs. [7, 8] and therefore for  $\nu = 9/4$  the first part of (20) which relates  $Q$  with the volume symmetry energy  $J$  and the isovector surface energy  $k_S$  constants, is identical to that

used in Refs. [7–10, 14, 15]. However, in our derivations  $\nu$  deviates from 9/4 and it is proportional to the function  $\mathcal{J}_-^2/g^2(w_r)$ . This function depends significantly on the SO interaction parameter  $\beta$  but not too much on the specific Skyrme forces. Indeed, the most sensitive parameter  $\mathcal{C}_-$  cancels in the expression (20) for  $\nu$ :  $k_S \propto \mathcal{C}_-$  and  $\tau \propto 1/c_{sym}^2 \propto \mathcal{C}_-$  [see also Eqs. (13) for  $k_S$ , (6) for  $c_{sym}$  and (18) for  $\tau$ ]. The constant  $\nu$  at  $\beta = 0$  can be easily evaluated,

$$\nu \approx \frac{108}{25} \frac{[1 - 8/(7c_{sym})]^2}{1 - 4/(3c_{sym})}, \quad (21)$$

with neglecting small terms  $\propto 1/c_{sym}^2$ ,  $c_{sym} \approx 2 - 6$  for the Skyrme parameters of Refs. [23, 24] [ $c_{sym} = \infty$  for T6 forces, see Eqs. (20), (14), (6) and (4) ( $w_r = 1/3$ ) and Table I]. Another difference in  $Q$  [Eq. (20)] from that of Refs. [7–10] is the expression (13) itself for  $k_S$ . Thus, the isovector stiffness coefficient  $Q$  introduced originally by Myers and Swiatecki [7, 8] is not a parameter of our approach but was found analytically in the explicit closed form (20) through the parameters of the Skyrme forces.

#### IV. DISCUSSION OF THE RESULTS

In Table II and also in Fig. 5 we show the isovector energy coefficient  $k_S$  [Eq. (13)], the stiffness parameter  $Q$  [Eq. (20)] and the neutron skin  $\tau$  [Eq. (18)] obtained within the ES approximation using the quadratic approximation for  $\epsilon(w)$  for several Skyrme forces [23, 24] with parameters presented in Table I. We also show the quantities  $k_{S0}$ ,  $\nu_0$ ,  $Q_0$  and  $\tau_0$  where the SO interaction is neglected ( $\beta = 0$ ). One can see a fairly good agreement for the analytical isoscalar energy constant  $b_S^{(+)}$  (12) with that of Refs. [23, 24] and [5] (Table I). The isovector energy coefficient  $k_S$  is more sensitive to the choice of the Skyrme forces than the isoscalar one  $b_S^{(+)}$  (Eq. (12) and Ref. [5]). The modulus of  $k_S$  is significantly larger for most of the Lyon Skyrme forces SLy [23] and SkI3 [24] than for the other ones. For these forces the stiffnesses  $Q$  are correspondingly smaller. The isovector stiffness  $Q$  is even more sensitive to the constants of the Skyrme force than the constants  $k_S$ . They are significantly larger for all forces, especially for SGII, than the well-known empirical values  $Q \approx 14 - 35$  MeV [8–10].

Swiatecki and his collaborators [9] found the stiffness  $Q \approx 14 - 20$  MeV by fitting the nuclear isovector giant dipole-resonance (IVGDR) energies calculated in the simplest version of the hydrodynamical model to the experimental data. Later, they suggested larger values  $Q \approx 30 - 35$  MeV accounting for a more detailed study of other phenomena in Refs. [8, 10]. In spite of several misprints in the derivations of the IVGDR energies in Ref. [9] (in particular, in Eq. (7.7) of [9] for the displacement of the center-of-mass conservation the factor  $NZ/A^2$  should be in the numerator

and not in the denominator of the irrotational flow moment of inertia (see Ref. [31]), the final result for the IVGDR energy constant is almost the same as for the asymptotically large values of  $Q$ ,  $3JA^{-1/3}/Q \ll 1$  ( $NZ/A^2 \approx 1/4$ ),

$$D = \hbar\omega_- A^{1/3} = D_\infty / \sqrt{1 + 3JA^{-1/3}/Q}, \quad D_\infty = \sqrt{8\hbar^2 J / (mr_0^2)}. \quad (22)$$

These values for  $D$  are in good agreement with the well-known experimental value  $D_{exp} \approx 80$  MeV for heavy nuclei ( $D \approx D_\infty \approx 88$  MeV) within a precision better or of the order of 20% (a little worse for the specific SkI3 Skyrme forces), as shown in Table II, see also Ref. [20] for a more proper HD approach and Refs. [32–34] for other semiclassical nuclear models taking all into account the nuclear surface motion. As shown in Ref. [6] the averaged IVGDR energies and the energy weighted sum rules (EWSR) obtained with the semiclassical FLD approach based on the Landau-Vlasov equation [22] with the macroscopic boundary conditions (see Appendix B) are also basically insensitive to the isovector surface energy constant  $k_S$ , and they are similarly in good agreement with the experimental data. An investigation of the splitting of the IVGDR within this approach into the main peak which exhausts mainly the independent-of-model EWSR and a satellite (with a much smaller contribution to the EWSR) focusing on a much more sensitive  $k_S$  dependence of the pygmy (IVGDR satellite) resonances (see Refs. [18, 19]) will be published elsewhere.

More precise  $A$ -dependence of the quantity  $D$  [Eq. (22)] for finite values of  $Q$  seems to be beyond the accuracy of these HD calculations because of several other reasons. More realistic self-consistent HF calculations accounting for the Coulomb interaction, surface-curvature and quantum-shell effects led to larger  $Q \approx 30 - 80$  MeV [4, 15]. With larger  $Q$  (see Table II) the fundamental parameter of the LDM expansion in Ref. [7],  $(9J/4Q)A^{-1/3}$ , is really small for  $A \gtrsim 40$ , and therefore, results obtained by using this expansion are more justified.

The most responsible parameter of the Skyrme HF approach leading in significant differences in the  $k_S$  and  $Q$  values is the constant  $\mathcal{C}_-$  in the gradient terms of the energy density [Eq. (2) and Table I]. Indeed, the key quantity in the expression for  $Q$ , Eq. (20), and the isovector surface energy constant  $k_S$  [or  $b_S^-$ , Eq. (13)], is the constant  $\mathcal{C}_-$  because one mainly has  $k_S \propto \mathcal{C}_-$  (see Fig. 5), and  $Q \propto 1/k_S \propto 1/\mathcal{C}_-$ . As seen in Table I and in Fig. 5 the constant  $\mathcal{C}_-$  is very different for the different Skyrme forces (even in sign). As shown in Fig. 3 and below Eq. (20), other quantities in Eq. (20) are much less sensitive to most Skyrme interactions. The situation is very much in contrast to the isoscalar energy density constant  $b_S^{(+)} \propto C_+$  [Eq. (12)]. All Skyrme parameters are fitted to the well-known experimental value  $b_S^{(+)} = 17 - 19$  MeV because  $\mathcal{C}_+$  is almost constant (Table I). Contrary to this, there are so far no clear experiments which would determine  $k_S$  well



enough because the mean energies of the IVGDR (main peaks) do not depend very much on  $k_S$  for the different Skyrme forces (see last two rows of Table II). Perhaps, the low-lying isovector collective states are more sensitive but there is no careful systematic study of their  $k_S$  dependence at the present time. Another reason for so different  $k_S$  and  $Q$  values might be traced back to the difficulties in deducing  $k_S$  directly from the HF calculations due to the curvature and quantum effects in contrast to  $b_S^{(+)}$ . We have also to go far away from the nuclear stability line to subtract uniquely the coefficient  $k_S$  in the dependence of  $b_S^{(-)} \propto I^2 = (N - Z)^2/A^2$ , according to Eq. (13). For exotic nuclei one has more problems to relate  $k_S$  to the experimental data with a good enough precision. Note that  $k_S$  is a more fundamental constant than the isovector stiffness  $Q$  due to the direct relation to the tension coefficient  $\sigma_-$  of the isovector capillary pressure. Therefore, it is simpler to analyze the experimental data for the IVGDR within the macroscopic HD or FLD models in terms of the constant  $k_S$ . The quantity  $Q$  involves also the ES approximation for the description of the nuclear edge through the neutron skin  $\tau$  [see Eq. (15)]. The precision of this description depends more on the specific nuclear models [14–17]. On the other hand, the neutron skin thickness  $\tau$  is interesting in many aspects for the investigation of exotic nuclei, in particular, in nuclear astrophysics.

We emphasize that for specific Skyrme forces there exists an abnormal behavior of the isovector surface constants  $k_S$  and  $Q$ . It is related to the fundamental constant  $\mathcal{C}_-$  of the energy density (2). For the parameter set T6 ( $\mathcal{C}_- = 0$ ) one finds  $k_S = 0$ . Therefore, according to Eq. (20), the value of  $Q$  diverges ( $\nu$  is almost independent on  $\mathcal{C}_-$ ). Notice that the isovector gradient terms which are important for the consistent derivations within the ES approach are also not included ( $\mathcal{C}_- = 0$ ) into the symmetry energy density in Refs. [11, 13]. Moreover, for RATP [23] and SkI [24] (also for the specific Skyrme forces BSk6 and BSk8 of Ref. [12]<sup>1</sup>), the isovector stiffness  $Q$  is even negative as  $\mathcal{C}_- > 0$  ( $k_S > 0$ ) in contrast to all other Skyrme forces.

Table II shows also the coefficients  $\nu$  of Eq. (20) for the isovector stiffness  $Q$ . They are mostly constant [ $\nu_0 \approx 2 - 4$ , see Eq. (21) and Table II] for all Skyrme forces at  $\beta = 0$ . However, these constants  $\nu$  are rather sensitive to the SO, i.e. to the  $\beta$  dependence of both the function  $g(w_r)$  [Eq. (19)] in the expression (18) for the neutron skin  $\tau$  and to the constant  $\mathcal{J}_-$  [Eq. (14)] in the expression (13) for the isovector energy coefficient  $k_S$ . As compared to 9/4 suggested in Ref. [7], they are significantly smaller in magnitude for the most of the Skyrme forces (besides of SGII and T6 with larger values of  $\nu$ ).

---

<sup>1</sup> Notice also that for the BSk forces [12] we found an unexpected behavior of the particle density  $w_-(x)$  with a negative minimum near the ES (a proton instead of neutron skin because of  $\rho_n < \rho_p$ , in contrast to any other forces discussed in Ref. [23] with  $w_-$  being always positive)

## V. CONCLUSIONS

Simple expressions for the isovector parts of the particle densities and energies in the leading ES approximation were used for the derivation of analytical expressions of the neutron skin thickness and the isovector stiffness coefficients. As shown in Appendix B we have to include higher order terms in the parameter  $a/R$ . These terms depend on the well-known parameters of the Skyrme forces. Results for the isovector surface energy constant  $k_S$ , the neutron skin thickness  $\tau$  and the stiffness  $Q$  depend in a sensitive way on the choice of the parameters for the Skyrme functional, especially on the parameter  $\mathcal{C}_-$  in the gradient terms of the density in the surface symmetry energy density of Eq. (2). The values of the isovector constants  $k_S$ ,  $\tau$  and  $Q$  depend also very much on the SO interaction constant  $\beta$ . The isovector stiffness constants  $Q$  are significantly larger than those found earlier for all desired Skyrme forces. The mean IVGDR energies and sum rules calculated in the HD [9, 20, 31] and FLD [6, 22] models for the most  $k_S$  values in Table II are in a fairly good agreement with the experimental data. For further perspectives, it would be worth to apply our results to the calculations of the pygmy resonances in the IVGDR strength within the FLD model [22] and the isovector low-lying collective states within the periodic orbit theory [35–37] which are expected to be more sensitive to the values of  $k_S$ . Our approach is helpful for further study of the effects in the surface symmetry energy because it gives the analytical expressions for the constants  $k_S$  and  $Q$  directly connected with a few critical parameters of the Skyrme interaction without using any fitting.

## Acknowledgements

Authors thank M. Brack, M. Brenna, V.Yu. Denisov, V.M. Kolomietz, J. Meyer, V.O. Nesterenko, M. Pearson, V.A. Plujko, X. Roca-Maza, A.I. Sanzhur, and X. Vinas for many useful discussions. One of us (A.G.M.) is also very grateful for a nice hospitality during his working visits of the National Centre for Nuclear Research in Otwock-Swierk of Poland. This work was partially supported by the Deutsche Forschungsgemeinschaft Cluster of Excellence Origin and Structure of the Universe ([www.universe-cluster.de](http://www.universe-cluster.de)).

## Appendix A: Solutions to the isovector Lagrange equation

The Lagrange equation for the variations of the isovector particle density  $\rho_-$  in the energy density (2) up to the leading terms in a small parameter  $a/R$  is given by [5]

$$\mathcal{C}_- \frac{\partial^2 \rho_-}{\partial \xi^2} + \frac{d}{d\rho_-} [\rho_+ \varepsilon_-(\rho_+, \rho_-)] = 0, \quad (\text{A1})$$

where  $\varepsilon_-$  is defined just below Eq. (2). We neglected here the higher order terms proportional to the first derivatives of the particle density  $\rho_-$  with respect to  $\xi$  and the surface correction to the isovector chemical potential like in Refs. [2, 3] for the isoscalar case. For the dimensionless isovector density  $w_- = \rho_-/(\bar{\rho}I)$  after simple transformations one finds the following equation and the boundary condition in the form

$$\frac{dw_-}{dw} = c_{sym} \sqrt{\frac{1+\beta w}{\epsilon(w)}} \sqrt{1 - \frac{w_-^2}{w^2}}, \quad w_-(1) = 1, \quad (\text{A2})$$

where  $\beta$  is the SO parameter defined below Eq. (3), see also Eq. (6) for  $c_{sym}$ . The above equation determines the isovector density  $w_-$  as a function of the isoscalar one  $w(x)$  [Eq. (3)]. In the quadratic approximation for  $\epsilon(w)$  one explicitly finds

$$x(w) = \sqrt{1+\beta} \ln \left[ \frac{(1-w) \left( 1 + (1+2\beta)w_r + 2\sqrt{(1+\beta)(1+\beta w_r)w_r} \right)}{(1-w_r) \left( 1 + (1+2\beta)w + 2\sqrt{(1+\beta)(1+\beta w)w} \right)} \right] + \sqrt{-\beta} [\arcsin(1+2\beta w) - \arcsin(1+2\beta w_r)], \quad (\text{A3})$$

where  $w_r$  is the solution of the boundary condition (4). Substituting  $w_- = w \cos\psi$  into Eq. (A2), and taking the approximation  $\epsilon = (1-w)^2$ , one has the following first order differential equation for a new function  $\psi(w)$ :

$$\frac{w(1-w)}{c_{sym}} \sin\psi \psi' = \sqrt{1+\beta w} \sin\psi - \frac{1-w}{c_{sym}} \cos\psi, \quad \psi(1) = 0. \quad (\text{A4})$$

The boundary condition for this equation is related to that of Eq. (A2) for  $w_-(w)$ . This equation looks more complicated because of the trigonometric nonlinear terms. However, it allows to obtain simple approximate and rather exact analytical solutions within standard perturbation theory. Indeed, according to Eqs. (A2) and (3) where we have did not express the  $x$ -dependence explicitly we note that  $w_- \propto w(x)$  is a sharply decreasing function of  $x$  within a small diffuseness region of the order of one in dimensionless units (Figs. 2-4). Thus, we may find the approximate solutions to the equation (A4) (with its boundary condition) in terms of a power expansion of a new function  $\tilde{\psi}(\tilde{w})$  in terms of a new small argument  $\tilde{w}$ ,

$$\tilde{\psi}(\tilde{w}) \equiv \psi(w) = \sum_{n=0}^{\infty} c_n \tilde{w}^n, \quad (\text{A5})$$

with unknown coefficients  $c_n$  and  $\tilde{w}$  defined in Eq. (6). Substituting the power series (A5) into Eq. (A4) one expands first the trigonometric functions into power series of  $\tilde{w}$  in accordance with the boundary condition in Eq. (A4). As usual, using standard perturbation theory, we obtain the system of algebraic equations for the coefficients  $c_n$  [Eq. (A5)] by equating the coefficients

from both sides of Eq. (A4) at the same powers of  $\tilde{w}$ . This simple procedure leads to a system of algebraic recurrence relations which determine the coefficients  $c_n$  as functions of the parameters  $\beta$  and  $c_{sym}$  of Eq. (A4),

$$\begin{aligned} c_0 &= 0, & c_1 &= \frac{1}{\sqrt{1+\beta}}, & c_2 &= \frac{c_1}{\sqrt{1+\beta}} \left( \frac{\beta c_{sym}}{2\sqrt{1+\beta}} - c_1 \right), \\ c_3 &= \frac{1}{\sqrt{1+\beta}} \left\{ \frac{\beta^2 c_{sym}^2 c_1}{8(1+\beta)^{3/2}} + c_1^2 \left( c_{sym} - \frac{1}{2} \right) + \frac{1}{6} \sqrt{1+\beta} c_1^3 + c_2 \left( \frac{\beta c_{sym}}{2\sqrt{1+\beta}} - 3c_1 \right) \right\}, \end{aligned} \quad (\text{A6})$$

etc. In particular, up to the second order in  $\tilde{w}$ , we derive an analytical solution in an explicitly closed form:

$$\tilde{\psi}(\tilde{w}) = \tilde{w} (c_1 + c_2 \tilde{w}), \quad c_1 = \frac{1}{\sqrt{1+\beta}}, \quad c_2 = \frac{1}{(1+\beta)^{3/2}} \left( \frac{\beta}{2} c_{sym} - 1 \right). \quad (\text{A7})$$

Thus, using the standard perturbation expansion method of solving  $\tilde{\psi}(\tilde{w})$  in terms of the power series of the  $\tilde{w}$  (up to  $\tilde{w}^2$ ), one obtains the quadratic expansion of  $\psi(w)$  [Eq. (7)] with  $\tilde{c} = c_2/c_1$ . Notice that one finds a good convergence of the power expansion of  $\tilde{\psi}(\tilde{w})$  (A7) in  $\tilde{w}$  for  $w_-(x)$  at the second order in  $\tilde{w}$  because of the large value of  $c_{sym}$  for all Skyrme forces presented in Table I [Eq. (6) for  $c_{sym}$ ].

## Appendix B: The macroscopic boundary conditions and surface tension coefficients

For the derivation of the expression for the surface tension coefficients  $\sigma_{\pm}$ , we first write the system of the Lagrange equations by using variations of the energy density  $\mathcal{E}(\rho_+, \rho_-)$  with respect to the isoscalar and isovector densities  $\rho_+$  and  $\rho_-$ . Then, we substitute the solution of the first Lagrange equation for the variations of the isoscalar density  $\rho = \rho_+$  in the energy density (2) (Refs. [2, 3]) into the second Lagrange equation for the isovector density  $\rho_-$ . Using the Laplacian in the variables  $\xi$  and  $\eta$  (Appendix A in Ref. [2]) we keep the major terms in this second equation within the improved precision in the small parameter  $a/R$ . The improved precision means that we take into account the next terms proportional to the first derivatives of the particle densities [along with the second ones of Eq. (A1)] and the small surface corrections  $\Lambda_{\pm}$  to the isoscalar and isovector Lagrange multipliers  $\lambda_{\pm}$ . Within this improved precision, one finds the second Lagrange equation by the variations of the energy density  $\mathcal{E}(\rho_+, \rho_-)$ , Eq. (2), with respect to the isovector particle density  $\rho_-$ :

$$\mathcal{C}_- \frac{\partial^2 \rho_-}{\partial \xi^2} + 2\mathcal{C}_- H \frac{\partial \rho_-}{\partial \xi} - \frac{d}{d\rho_-} [\rho_+ \varepsilon_-(\rho_+, \rho_-)] + \Lambda_- = 0, \quad (\text{B1})$$

where  $H$  is the mean curvature of the ES ( $H = 1/R$  for the spherical ES). The isovector chemical-potential correction  $\Lambda_-$  was introduced [5] like the isoscalar one  $\Lambda_+$  worked out in details in Refs.

[2, 3]. Multiplying Eq. (B1) by  $\partial\rho_-/\partial\xi$  we integrate in the coordinate  $\xi$  normal to the ES from a spatial point  $\xi_{in}$  inside the volume (at  $\xi_{in} \lesssim -a$ ) to  $\infty$  term by term. Using also the integration by parts, within the ES approximation it results in the macroscopic boundary conditions (together with the isoscalar condition from [2, 3, 5, 22, 29, 30]):

$$(\bar{\rho} I \Lambda_-)_{ES} = P_s^{(-)} \equiv 2\sigma_- H, \quad (\bar{\rho} \Lambda_+)_{ES} = P_s^{(+)} \equiv 2\sigma_+ H. \quad (B2)$$

Here,  $P_s^{(\pm)}$  are the isovector and isoscalar surface-tension (capillary) pressures and  $\sigma_{\pm}$  are the corresponding tension coefficients [see their expressions in Eq. (8)]. The Lagrange multipliers  $\Lambda_{\pm}$  multiplied by  $\bar{\rho}I$  and  $\bar{\rho}$  in the circle brackets on the left hand sides of equations (B2) are the volume isovector ( $\bar{\rho}I\Lambda_-$ ) and isoscalar ( $\bar{\rho}\Lambda_+$ ) pressure excesses, respectively (see Ref. [5]). These pressures due to the surface curvature can be derived using the volume solutions of the Lagrange equations for the particle densities [obtained by doing variations of the energy density  $\mathcal{E}$  and neglecting all the derivatives of the particle densities in Eq. (2)],

$$\rho_- \approx \bar{\rho} \left[ I \left( 1 + \frac{9\Lambda_+}{K} \right) + \frac{\Lambda_-}{2J} \right], \quad \rho_+ \approx \bar{\rho} \left[ 1 + \frac{9\Lambda_+}{K} \left( 1 - \frac{81\Lambda_+}{2K} \right) - \frac{18J}{2K} I^2 \right]. \quad (B3)$$

Inserting  $\Lambda_+$  and  $\Lambda_-$  from Eq. (B2) into Eq. (B3) one gets

$$\rho_- = \bar{\rho} I \left[ 1 + \frac{6b_S^{(+)} H r_0}{K} + \frac{2b_S^{(-)} H r_0}{6J I^2} \right]. \quad (B4)$$

As seen from Eq. (B4), the isovector density correction to the volume density  $\rho_-$  due to a finiteness of the coupled system of the two Lagrange equations depend on both isoscalar and isovector surface energy constants  $b_S^{(\pm)}$  in the first order expansion of the small parameter  $a/R$ . If we are not too far from the valley of stability  $I$  is an additional small parameter and the isovector corrections are small as compared with the isoscalar values [ $b_S^{(-)} \propto I^2$ ,  $\Lambda_- \propto I$ , see Eqs. (B3), (B4) and (13)]. Thus, Eq. (B2) has a clear physical meaning as the macroscopic boundary conditions for equilibrium of the isovector and isoscalar forces (volume and surface pressures) acting on the ES [22, 28]. Note that in these derivations we used Eq. (A1) in leading order in  $a/R$  [neglecting small terms proportional to the first derivative  $\partial\rho_-/\partial\xi$  and  $\Lambda_-$  in Eq. (B1)], like for the isoscalar case considered in Refs. [2, 3, 29, 30]. The obvious boundary conditions of disappearance of the particle densities and all their derivatives with respect to  $\xi$  outside of the ES for  $\xi \rightarrow \infty$  ( $\xi \gg a$ ) were taken into account too. The isovector tension coefficient  $\sigma_-$  is much smaller than the isoscalar one  $\sigma_+$  [see Eq. (8)] as  $\sigma_- \propto I^2$  due to  $\rho_- \propto I$  and  $I \ll 1$  is small near the nuclear stability line. Another reason is also because of a smallness of  $\mathcal{C}_-$  as compared to  $\mathcal{C}_+$  for the realistic Skyrme forces [23, 24]. From comparison of Eqs. (B3) and (B4) for  $\rho_-$  [see also Eq. (8)], one may evaluate

$$\frac{\Lambda_-}{e_F} = \frac{2\sigma_- H}{\bar{\rho} e_F I} \approx \frac{2b_S^{(-)}}{e_F I A^{1/3}} \sim I \frac{a}{R}. \quad (B5)$$

which is consistent with Eq. (B1) ( $r_0 H \sim a/R$  in these estimations, see corresponding ones in Refs. [2, 3]).

### Appendix C: Derivations of the surface energy and its coefficients

For calculations of the surface energy components  $E_S^{(\pm)}$  of the energy  $E$ , Eq. (1), within the same improved ES approximation as described above in Appendix B we first may separate the volume terms related to the first two terms of Eq. (2) for the energy density  $\mathcal{E}$ . Other terms of the energy density  $\mathcal{E}(\rho_+, \rho_-)$  in Eq. (2) lead to the surface components  $E_S^\pm$  [Eq. (11)], as they are concentrated near the ES. Integrating the energy density  $\mathcal{E}$  [see Eq. (2)] over the spatial coordinates  $\mathbf{r}$  in the local coordinate system  $\xi, \eta$  (see Fig. 1) in the ES approximation one finds

$$E_S^\pm = \mathcal{C}_\pm \oint d\mathcal{S} \int_{\xi_{in}}^\infty d\xi [(\nabla \rho_\pm)^2 - \rho_+ \varepsilon_\pm(\rho_+, \rho_-)] \approx \sigma_\pm \mathcal{S}, \quad (\text{C1})$$

where  $\xi_{in} \lesssim -a$  is like in Appendix B [2, 3, 5]. The local coordinates  $\xi, \eta$  were used because the integral over  $\xi$  converges rapidly within the ES layer which is effectively taken for  $|\xi| \lesssim a$ . Therefore, we may extend formally  $\xi_{in}$  to  $-\infty$  in the first (internal) integral taken over the ES in the normal direction  $\xi$  in Eq. (C1). Then, the second integration is performed over the closed surface of the ES. The integrand over  $\xi$  contains terms of the order of  $(\bar{\rho}/a)^2 \propto (R/a)^2$  like the ones of the leading order in Eq. (B1) [see for instance the second derivatives in Eq. (A1) which are also  $\propto (R/a)^2$ ]. However, the integration is effectively performed over the edge region of the order of  $a$  that leads to the additional smallness proportional to  $a/R$ . At this leading order the  $\eta$  dependence of the internal integrand can be neglected. Moreover, from the Lagrange equations at this order one can realize that the terms without the particle density gradients in Eq. (C1) are equivalent to the gradient terms. Therefore, for the calculation of the internal integral we may approximately reduce the integrand over  $\xi$  to the only derivatives of the particle densities of the leading order  $\rho_\pm(\xi)$  in  $\xi$  (with the factor 2) using  $(\nabla \rho_\pm)^2 - \rho_+ \varepsilon_\pm(\rho_+, \rho_-) \approx 2(\partial \rho_\pm / \partial \xi)^2$  [see Eqs. (3) and (7)]. Taking the integral over  $\xi$  within the infinite integration region ( $-\infty < \xi < \infty$ ) off the integral over the ES ( $d\mathcal{S}$ ) we are left with the integral over the ES itself that is the surface area  $\mathcal{S}$ . Thus, we arrive finally at the r.h.s. of Eq. (C1) with the surface tension coefficient  $\sigma_\pm$  [Eq. (8)].

Using now the quadratic approximation  $\epsilon(w) = (1 - w)^2$  in Eq. (8) for  $b_S^\pm = 4\pi r_0^2 \sigma_\pm$  ( $\mathcal{D}_- = 0$ ) one obtains (for  $\beta < 0$ , see Table I)

$$b_S^{(\pm)} = 6\bar{\rho} \mathcal{C}_\pm \mathcal{J}_\pm / (r_0 a), \quad (\text{C2})$$

where

$$\begin{aligned} \mathcal{J}_+ &= \int_0^1 dw \sqrt{w(1+\beta w)} (1-w) = \frac{1}{24} (-\beta)^{-5/2} \left[ \mathcal{J}_+^{(1)} \sqrt{-\beta(1+\beta)} \right. \\ &\quad \left. + \mathcal{J}_+^{(2)} \arcsin \sqrt{-\beta} \right], \quad \mathcal{J}_+^{(1)} = 3 + 4\beta(1+\beta), \quad \mathcal{J}_+^{(2)} = -3 - 6\beta. \end{aligned} \quad (\text{C3})$$

For the isovector energy constant  $\mathcal{J}_-$  one finds

$$\begin{aligned} \mathcal{J}_- &= -\frac{1}{1+\beta} \int_0^1 dw \sqrt{w(1+\beta w)} (1-w)(1+\tilde{c}\tilde{w})^2 \\ &= \frac{\tilde{c}^2}{1920(1+\beta)(-\beta)^{9/2}} \left[ \mathcal{J}_-^{(1)} (c_{sym}/\tilde{c}) \sqrt{-\beta(1+\beta)} + \mathcal{J}_-^{(2)} (c_{sym}/\tilde{c}) \arcsin \sqrt{-\beta} \right], \\ \mathcal{J}_-^{(1)}(\zeta) &= 105 - 4\beta \{ 95 + 75\zeta + \beta [119 + 10\zeta(19 + 6\zeta) + 8\beta^2(1 + 10\zeta(1 + \zeta)) \\ &\quad + 8\zeta(5\zeta(3 + 2\zeta) - 6)] \}, \\ \mathcal{J}_-^{(2)}(\zeta) &= 15 \{ 7 + 2\beta [5(3 + 2\zeta) + 8\beta(1 + \zeta)(3 + \zeta + 2\beta(1 + \zeta))] \}. \end{aligned} \quad (\text{C4})$$

These equations determine explicitly the analytical expressions for the isoscalar ( $b_S^+$ ) and isovector ( $b_S^-$ ) energy constants in terms of the Skyrme force parameters, see Eqs. (7) for  $\tilde{c}$ , (6) for  $c_{sym}$  and  $\tilde{w}$ . For the limit  $\beta \rightarrow 0$  from Eqs. (C3) and (C4) one has  $\mathcal{J}_\pm \rightarrow 4/15$ . With Eqs. (18) and (19) one arrives also at the explicit analytical expression for the isovector stiffness  $Q$  as a function of  $\mathcal{C}_-$  and  $\beta$ . In the limit  $\mathcal{C}_- \rightarrow 0$  one obtains  $k_S \rightarrow 0$  and  $Q \rightarrow \infty$  because of the finite limit of the argument  $c_{sym}/\tilde{c} \rightarrow (1+\beta)/\beta$  of the function  $\mathcal{J}_-$  in Eq. (C4) [see also Eqs. (7) for  $\tilde{c}$  and (6) for  $c_{sym}$ ].

- 
- [1] V.M. Strutinsky and A.S. Tyapin, Exp. Theor. Phys. (USSR) **18**, 664 (1964).
  - [2] V.M. Strutinsky, A.G. Magner, and M. Brack, Z. Phys., A **319**, 205 (1984).
  - [3] V.M. Strutinsky, A.G. Magner, and V. Yu. Denisov, Z. Phys., A **322**, 149 (1985).
  - [4] M. Brack, C. Guet, and H.-B. Hakansson, Phys. Rep. **123**, 275 (1985).
  - [5] A.G. Magner, A.I. Sanzhur, and A.M. Gzhebinksky, Int. J. Mod. Phys. E **18**, 885 (2009).
  - [6] J.P. Blocki, A.G. Magner, and A.A. Vlasenko, Nucl. Phys. and At. Energy, **13**, No 4 (2012).
  - [7] W.D. Myers, W.J. Swiatecki, Ann. Phys. **55**, 395 (1969); *ibid* **84**, 186 (1974).
  - [8] W.D. Myers, W.J. Swiatecki, Nucl. Phys. A **336**, 267 (1980); *ibid* Phys. Rev. C **601**, 141 (1996).
  - [9] W.D. Myers et al., Phys. Rev. C **15**, 2032 (1977).
  - [10] W.D. Myers, W.J. Swiatecki, and C.S. Wang, Nucl. Phys. A **436**, 185 (1985).
  - [11] P. Danielewicz, Nucl. Phys. A **727**, 233 (2003).
  - [12] M. Samyn, S. Gorily, M. Bender, and J.M. Pearson, Phys. Rev. C, **70**, 044309 (2004).

- [13] P. Danielewicz, J. Lee, Int. J. Mod. Phys. E **18**, 892 (2009).
- [14] M. Centelles, X. Roca-Maza, X. Vinas, and M. Warda, Phys. Rev. Lett., **102**, 012502 (2009).
- [15] M. Warda, X. Vinas, X. Roca-Maza, and M. Centelles, Phys. Rev. C **81**, 054309 (2010); *ibid* **82**, 054314 (2010)
- [16] M. Warda, X. Vinas, X. Roca-Maza, and M. Centelles, Phys. Rev. C **82**, 054314 (2010).
- [17] X. Roca-Maza, M. Centelles, X. Vinas, and M. Warda, Phys. Rev. Lett. **106**, 252501 (2011).
- [18] S. Siem, Small resonances on the tail of the giant dipole resonances, 4th Int. Conf. Current Problems in Nuclear Physics and Atomic Energies, NPAE-Kyiv 2012, Sept. 3-7.
- [19] A. Repko, R.-G. Reinhard, V.O. Nesterenko, and J. Kvasil, preprint, arXiv: 1212.2088v1 [nucl-th], in press of the PRC, 2013.
- [20] V.Yu. Denisov, Sov. J. Nucl. Phys. **43**, 28 (1086).
- [21] V.M. Kolomietz and A.G. Magner, Phys. Atom. Nucl. **63**, 1732 (2000).
- [22] V.M. Kolomietz, A.G. Magner, and S. Shlomo, Phys. Rev. C **73**, 024312 (2006).
- [23] E. Chabanat et al., Nucl.Phys. A **627**, 710 (1997); *ibid* **635**, 231 (1998).
- [24] R.-G. Reinhard and H. Flocard, Nucl. Phys. A **585**, 467 (1995).
- [25] M. Bender, P.-H. Heenen, P.-G. Reinhard, Rev. Mod. Phys. **75**, 121 (2003).
- [26] J.R. Stone, R.-G. Reinhard, Prog. Part. Nucl. Phys. **58**, 587 (2007).
- [27] J.Erler, C.J. Horowitz, W. Nazarevich, M. Rafalski, and P.-G. Reinhard, arXiv:1211.6292v1 [nucl-th] 27 Nov. 2, 2012.
- [28] Aa. Bohr and B. Mottelson, *Nuclear structure* (W.A. Benjamin, New York, 1975), Vol. II.
- [29] A.G. Magner, V.M. Strutinsky, Z. Phys. A **322**, 149 (1985); Sov. J. Nucl. Phys. **44**, 591 (1986).
- [30] A.G. Magner, Sov. J. Nucl. Phys. **45**, 235 (1987) [Yad. Fiz. **45**, 374 (1987).
- [31] J.M. Eisenberg, W. Greiner, *Nuclear Theory, Vol. 1, Nuclear Models Collective and Single-Particle Phenomena* (North-Holland Publishing Company Amsterdam-London, 1970).
- [32] V.A. Plujko, O.M. Gorbachenko, R. Capote, and V.M. Bondar, Proc. of the 3rd Int. Conf. “Current problems in Nuclear Physics and Atomic Energy (Kyiv, Ukraine, June 7-12, 2010), part 1, Kyiv, 342 (2011).
- [33] V.A. Plujko, O.M. Gorbachenko, V.M. Bondar, and R. Capote, J. of the Korean Physical Society, **59**, 1514 (2011).
- [34] V.A. Plujko, R. Capote, and O.M. Gorbachenko, **97**, 567 (2011).
- [35] A.M. Gzhebinsky, A.G. Magner, S.N. Fedotkin, Phys. Rev. C **76**, 064315 (2007).
- [36] J.P. Blocki, A.G. Magner and I.S. Yatsyshyn, Int. Journ. Mod. Phys. E **21**, 1250034 (2012).



- [37] J.P. Blocki and A.G. Magner, IX Int. Nuclear Physics Workshop "Maria & Pierre Curie", 26-30th Sept., 2012, Kazimierz Dolny, Poland; Physica Scripta, in press, 2013 .

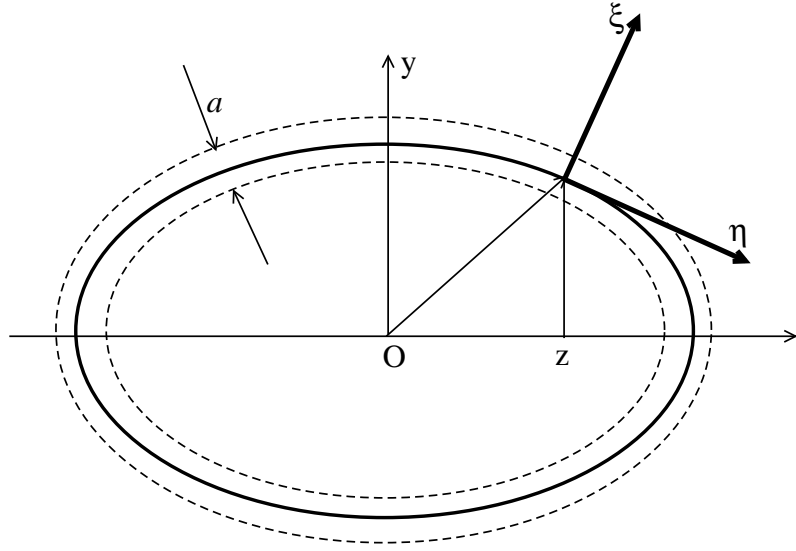


FIG. 1. The ES and local  $\xi, \eta$  coordinates. The ES in the cylindrical  $y, z$  coordinates with the symmetry axis  $z$  and diffuseness parameter  $a$  are shown schematically by the thick solid and dashed curves (after Ref. [5]).

	SkM*	SkM	SIIM	SGII	RATP	SkP	T6	SkI3	SLyb	SLy4	SLy5	SLy6	SLy7
$\bar{\rho}$ , fm <sup>-3</sup>	0.16	0.16	0.15	0.16	0.16	0.16	0.16	0.16	0.16	0.16	0.16	0.17	0.16
$b_V$ , MeV	15.8	15.8	15.9	15.6	16.0	15.9	16.0	16.0	16.0	16.0	16.0	16.0	16.0
$K$ , MeV	217	217	355	215	240	201	236	258	230	230	230	230	230
$J$ , MeV	30.1	31.0	28.2	26.9	29.3	30.0	30.0	34.8	32.0	32.0	32.1	31.9	31.9
$C_+$ , MeV·fm <sup>5</sup>	57.6	52.9	49.4	43.9	60.2	60.1	55.1	51.8	59.5	59.5	59.3	54.0	52.7
$C_-$ , MeV·fm <sup>5</sup>	-4.79	-4.69	-5.59	-0.94	13.9	-20.2	0	12.6	-22.3	-22.3	-22.8	-15.6	-13.4
$a$ fm	0.52	0.50	0.59	0.45	0.55	0.50	0.52	0.53	0.53	0.53	0.53	0.52	0.50
$a_d$ fm	0.63	0.58	0.73	0.58	0.71	0.71	0.70	0.63	0.68	0.68	0.68	0.61	0.61
$c_{sym}$	3.26	3.21	3.42	6.02	2.00	1.52	$\infty$	2.20	1.59	1.59	1.57	1.80	1.93
$\beta$	-0.64	-0.69	-0.57	-0.54	-0.52	-0.37	-0.45	-0.65	-0.55	-0.55	-0.58	-0.59	-0.65
$b_S^+$ , MeV [23, 24]	16.0	16.0	17.0	14.8	17.9	17.9	17.9	16.0	16.7	18.1	18.0	17.4	17.0
$b_S^+$ , MeV	21.2	19.9	14.5	18.7	21.7	24.9	21.3	18.3	21.7	21.7	21.5	21.6	19.6

TABLE I. Basic parameters of the Skyrme forces from Refs. [23, 24] and the isoscalar surface energy constants  $b_S^{(+)}$  of Eq. (12); the critical parameters  $a$  [Eq. (3)] and  $a_d$  [Eq. 5] for the nuclear diffuseness edge, the isoscalar and isovector constants  $C_{\pm}$  of the energy density [Eq. (2)],  $c_{sym}$  [Eq. (6)] and the spin-orbit constant  $\beta$  [see below Eq. (3)]; SLyb denotes shortly SLy230b of Ref. [23].

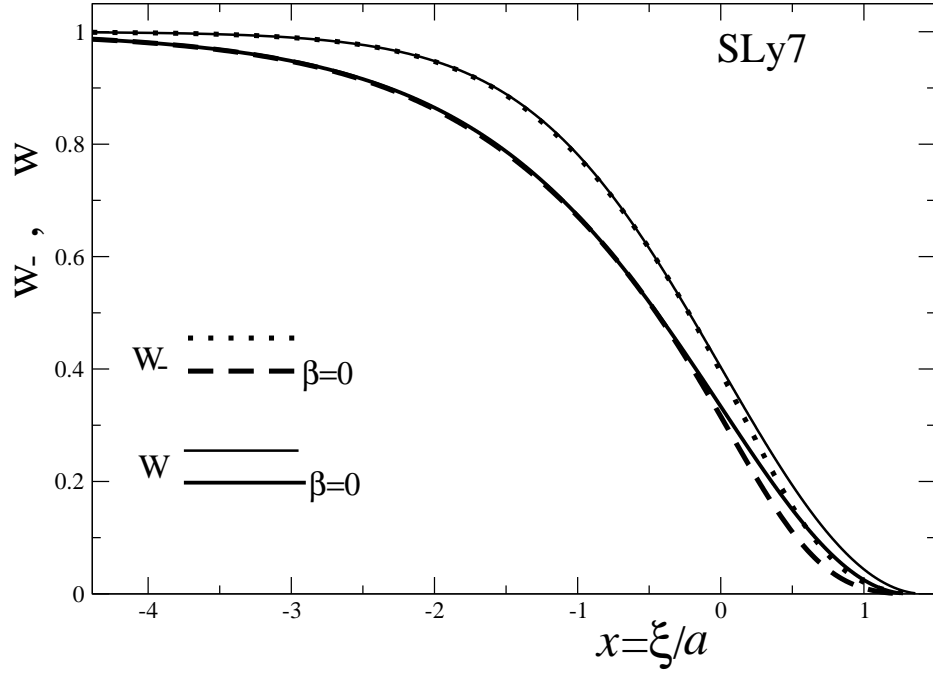


FIG. 2. Isoscalar  $w$  [see Eqs. (3), (A3)] and isovector  $w_-$  [Eq. (7)] particle densities vs  $x = \xi/a$  with and without ( $\beta = 0$ ) SO terms for the Skyrme force SLy7 as a typical example like in Ref. [5].

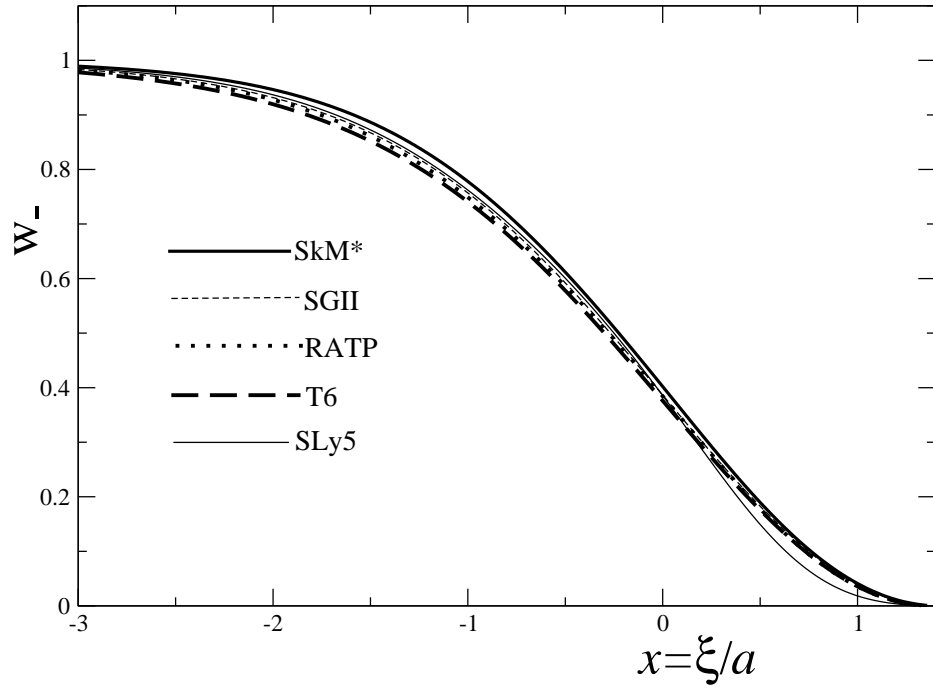


FIG. 3. Isovector particle densities  $w_-(x)$  (7) as functions of  $x$  within the quadratic approximation to  $\epsilon(w)$  for several Skyrme forces [23], see also Ref. [5].

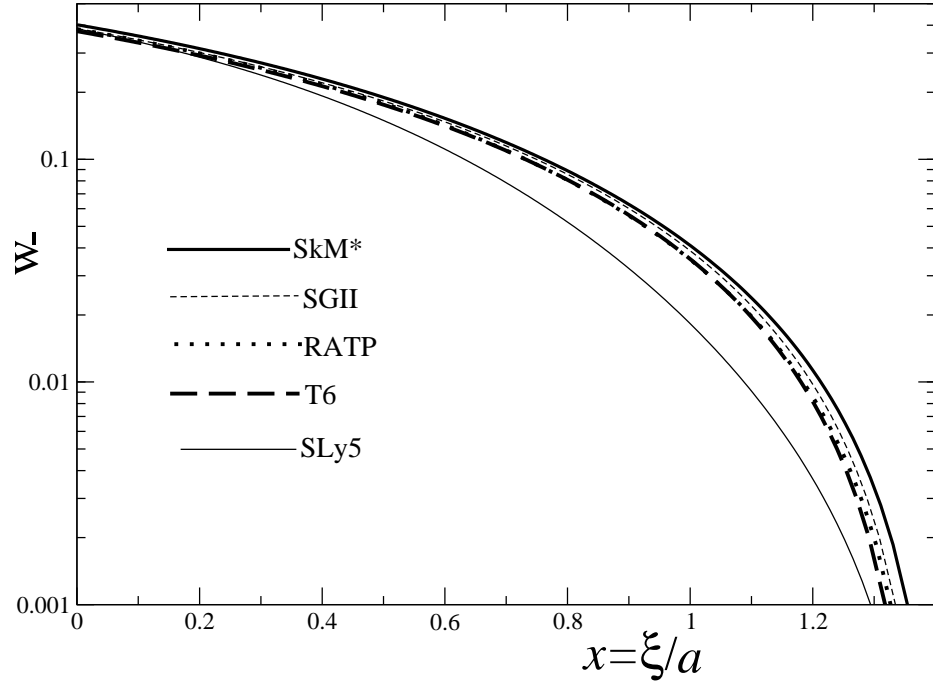


FIG. 4. The same as in Fig. 3 for the critical Skyrme interactions but within a smaller edge diffuseness region in the logarithmic scale.

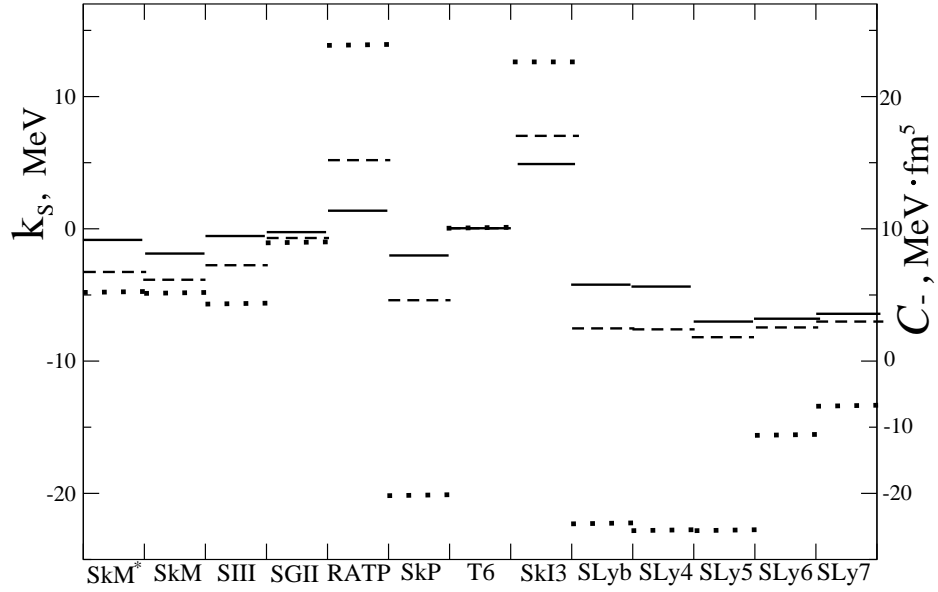


FIG. 5. Isovector energy constant  $k_S$  Eq. (13) (solid bars, left axis) vs the coefficient  $C_-$  (dotted points, right scale) of Eq. (2);  $k_{s,0}$  (dashed bars) is given by Eq. (13) without the spin-orbit interaction ( $\beta = 0$ ).

	SkM*	SkM	SIIM	SGII	RATP	SkP	T6	SkI3	SLyb	SLy4	SLy5	SLy6	SLy7
$k_{S,0}$ , MeV	-3.26	-3.84	-2.65	-0.71	5.25	-5.36	0	6.93	-7.51	-7.54	-8.14	-7.45	-6.95
$k_S$ , MeV	-0.77	-1.90	-0.52	-0.21	1.42	-1.93	0	4.88	-4.24	-4.38	-6.96	-6.72	-6.32
$\nu_0$	3.08	3.06	3.14	3.64	2.38	2.17	4.32	2.53	2.12	2.12	2.12	2.22	3.32
$\nu$	0.34	0.46	1.42	17.9	0.45	1.76	4.30	0.56	0.44	0.44	0.59	0.65	0.67
$Q_0$ , MeV	7744	9487	6255	16879	-371	3815	$\infty$	-6314	4771	4794	5178	5350	5703
$Q$ , MeV	398	234	2168	60998	-270	823	$\infty$	-140	105	104	87	98	109
$\tau_0/I$	0.021	0.020	0.021	0.0065	0.038	0.037	0	0.033	0.040	0.40	0.040	0.037	0.035
$\tau/I$	0.044	0.090	0.015	0.0019	0.072	0.048	0	0.187	0.20	0.21	0.28	0.26	0.24
$D_{HD}$ , MeV	85-86	85-86	82	82	90-89	87	88	105-100	81-84	81-84	79-83	81-85	81-84
$D_{FLD}$ , MeV	73-82	71-76	79-104	74-77	77-87	70-69	86-88	101-106	80-90	80-90	76-84	80-91	77-89

TABLE II. Isovector energy  $k_S$  and stiffness  $Q$  coefficients are shown for several Skyrme forces [23, 24];  $\nu$  is the constant of Eq. (20);  $\tau/I$  is the neutron skin calculated by Eq. (18); quantities  $k_{S,0}$ ,  $\nu_0$ ,  $Q_0$  and  $\tau_0$  are calculated with  $\beta = 0$ ; the intervals of monotonic functions  $D_{HD}(A)$  and  $D_{FLD}(A)$  for the HD and FLD models in the last two lines are related to  $A \approx 50 - 200$  (the last line is taken from Ref. [6]).